

## Rotating Instability in Low-Temperature Magnetized Plasmas

Jean-Pierre Boeuf<sup>1,2</sup> and Bhaskar Chaudhury<sup>1</sup>

<sup>1</sup>*Université de Toulouse, UPS, INPT; LAPLACE (Laboratoire Plasma et Conversion d'Énergie),  
118 route de Narbonne, F-31062 Toulouse cedex 9, France*

<sup>2</sup>*CNRS, LAPLACE, F-31062 Toulouse, France*

(Received 23 August 2013; published 11 October 2013)

The formation of a rotating instability associated with an ionization front (“rotating spoke”) and driven by a cross-field current in a cylindrical magnetized plasma is shown and explained for the first time on the basis of a fully kinetic simulation. The rotating spoke is a strong double layer (electrostatic sheath) moving towards the higher potential region at a velocity close to the critical ionization velocity, a concept proposed by Alfvén in the context of the formation of the solar system. The mechanisms of cross-field electron transport induced by this instability are analyzed.

DOI: [10.1103/PhysRevLett.111.155005](https://doi.org/10.1103/PhysRevLett.111.155005)

PACS numbers: 52.25.Xz, 52.20.-j, 52.35.Mw, 52.35.Ra

In many discharge devices operating at low pressure, a magnetic field  $B$  perpendicular to the discharge current is used to increase the residence time of electrons, allowing plasma sustainment by electron impact ionization, while ions can be accelerated collisionlessly in the applied electric field  $E$ . The  $E \times B$  configuration in these plasmas is very favorable for the formation of instabilities leading to “anomalous,” i.e., noncollisional electron transport across the magnetic field. Although plasma transport across a magnetic field is a central question and has attracted much attention in the context of fusion plasmas, little is known about  $E \times B$  instabilities in low-temperature discharge devices.

In this Letter we consider a generic plasma configuration where a current is driven through a magnetized plasma by applying a constant voltage between two concentric cylindrical electrodes in a uniform axial magnetic field. The magnetic field intensity is supposed to be such that electrons are magnetized (electron Larmor radius  $r_{ce}$  much smaller than electrode gap  $d$ ) while ions are not ( $r_{ci} > d$ ). As in most  $E \times B$  discharges, the geometry allows (azimuthal) closed drift to ensure efficient electron confinement. High-power plasma devices in a similar geometry were the subject of extensive experimental work in the 1960s–1980s focusing on the critical ionization velocity concept introduced by Alfvén [1] in his theory of the solar system, or in the context of fusion applications (see, e.g., the reviews by Piel *et al.* [2] and by Brenning [3]). An important conclusion of all these experiments was that the potential drop that can be maintained through a quasineutral magnetized plasma is limited to a value close to  $\delta U_p = v_c B d$ , where  $B$  is the magnetic field intensity,  $d$  is the electrode gap, and  $v_c$  is the critical ionization velocity (CIV) defined by  $v_c = \sqrt{2eU_i/M}$ , where  $U_i$  is the ionization potential of the gas and  $M$  the ion mass. Moreover, the experiments showed evidence of the presence of an instability rotating around the symmetry axis at the critical velocity and that can be associated with an  $E \times B$  rotation since

$v_c = \delta U_p / B d = E_r / B$ , where  $E_r$  is the radial plasma field. Piel, Möbius, and Himmel [4] proposed an inhomogeneous model where an azimuthal ionization front was associated with a sheath electric field rotating at the critical velocity. The azimuthal electric field  $E_\theta$  induces an electron drift  $E_\theta / B$  (secondary drift) along the sheath and Piel, Möbius, and Himmel [4], following others, suggested that this radial electron flow was subject to a two stream instability providing the energy necessary to ionize the gas in the azimuthal sheath and to maintain the front. This instability transforms the ion drift energy into random electron energy. Therefore ionization becomes possible when the ion drift energy reaches the ionization threshold, hence the CIV concept.

These experiments have been considered as a confirmation of the critical ionization velocity introduced by Alfvén [1] in the very different context of space plasmas and formation of the solar system. Alfvén conjectured that when the velocity of a neutral gas cloud, falling (due to gravity) in the magnetized plasma of the solar system reaches the critical velocity given above, rapid ionization occurs and an ionization front forms. After being ionized, the gas cloud is trapped by the magnetic field, and thus stopped from falling further in the gravitational field. Gas clouds of different masses would be trapped at different distances from the Sun, leading to the formation of planets.

The CIV phenomenon has been demonstrated in different experiments [2,3] where a plasma and a neutral gas are in relative motion across a magnetic field. Such conditions were created in gas-plasma impact experiments (plasma accelerated in a gas) and in the cross-field experiments (inducing a plasma rotation in the gas at rest) mentioned above.

We consider here a laboratory low-temperature magnetized plasma generated between two concentric cylinders by applying a dc voltage (cylindrical magnetron discharge; see the recent paper by Brenning *et al.* [5] for a discussion of rotating instabilities in high-power magnetron discharges and their relation to CIV). As in standard glow

discharges, the plasma is sustained by electron impact ionization in the volume combined with secondary electron emission at the cathode surface. A large part of the applied voltage is distributed in a sheath around the cathode, but, because of the strong electron magnetization and the resulting low electron conductivity, a non-negligible potential drop inside the quasineutral plasma is expected. This potential drop should increase with the Hall parameter  $h$  (ratio of the electron cyclotron angular frequency to the electron collision frequency,  $h = \omega_{ce}/\nu$ ). We have used a particle-in-cell (PIC) Monte Carlo collision (MCC) model [6] to describe this magnetized plasma, first in a one-dimensional (1D) electrode configuration, and in a 2D geometry. The conditions are argon, pressure in the 2–20 mtorr range, cathode radius  $R_1 = 0.5$  cm, anode radius  $R_2 = 2.5$  cm, magnetic field in the 10–40 mT range, applied voltage between 300 and 500 V, and secondary electron emission due to ion impact  $\gamma = 0.12$ . In these conditions the plasma density is on the order of  $10^{16} \text{ m}^{-3}$ , i.e., low enough for the PIC MCC simulations to be tractable, and collisions between charged particles and neutral atoms are dominant. The electron-argon collisions cross sections are those of Phelps [7], and a constant charge exchange collision cross section of  $8 \times 10^{-19} \text{ m}^2$  is assumed for ions.

The 1D simulation results of Fig. 1 predict that the potential drop inside the plasma increases with increasing Hall parameter. The plasma electric field at low pressure or large magnetic fields must increase and adjust to ensure electron transport to the anode in spite of the low electron mobility, and to generate through ionization the ions that are necessary to maintain quasineutrality. These results are in agreement with those of van der Straaten *et al.* [8]. 1D simulations are limited since they cannot describe instabilities in the  $E \times B$  or  $B$  directions. Moreover, an interesting feature of the results of Fig. 1 is that the electric field in the plasma and the plasma density gradients are in the same direction. This situation is known to be unstable, this instability being referred to as the Simon-Hoh or modified Simon-Hoh instability [9–11] in the

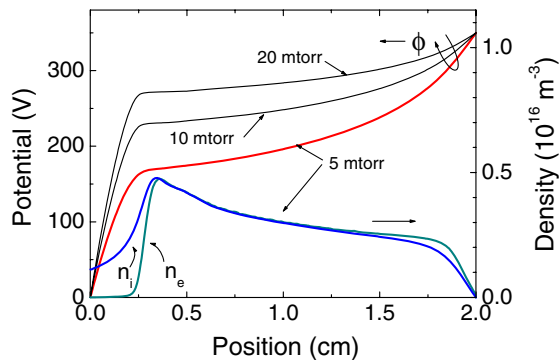


FIG. 1 (color online). Radial distribution of the charged particle densities and potential from a 1D PIC MCC simulation of a cylindrical magnetron discharge in argon. The position is indicated from the cathode surface (radius  $R_1 = 0.5$  cm).

literature. The Simon-Hoh instability is due to the difference in the electron and ion  $E \times B$  velocities that can arise because of the presence of collisions or because ions are less magnetized than electrons.

We performed 2D PIC MCC simulations in a plane perpendicular to the uniform magnetic field in the same conditions as Fig. 1. The 2D simulations confirm that these conditions are not stable and that the system evolves toward a solution exhibiting a rotating ionization front (rotating spoke [5]) and an associated azimuthal electrostatic sheath (double layer). Figure 2 shows the space distribution of the main plasma parameters at a given time. We see in Fig. 2(a) that the plasma potential is close to the anode voltage (350 V) in a region extending over an azimuthal angle of about  $3\pi/2$  and that the radial potential gradient in this region is small, in contrast with the 1D results of Fig. 1.

The potential is below the anode potential by about 25–30 V in the rest of the plasma, a region extending over an azimuthal angle of about  $\pi/2$ . Potential gradients are present at the two boundaries between the two regions,

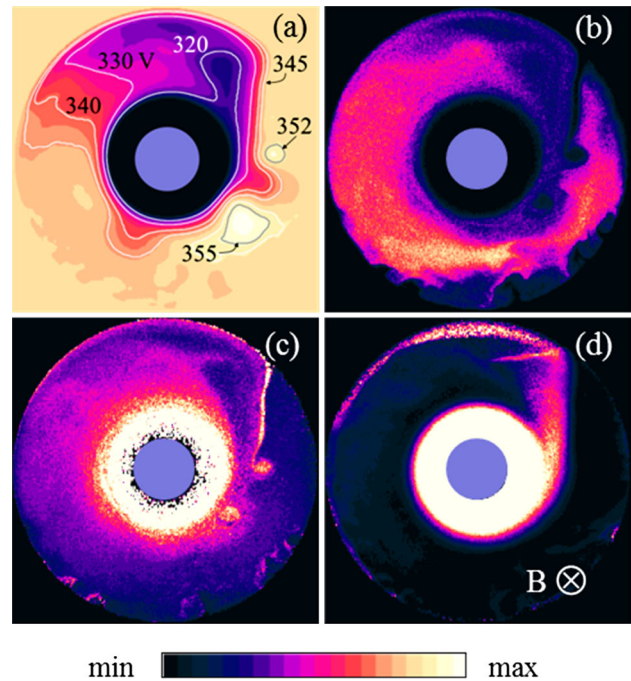


FIG. 2 (color online). Space distribution, at a given time of the 2D PIC MCC simulation, of (a) the electric potential, (b) the electron density, (c) the electron mean kinetic energy, and (d) the ion mean energy. The magnetic field is perpendicular to the simulation plane (downward). The conditions are argon, 10 mtorr, cathode diameter 1 cm, anode diameter 5 cm, magnetic field 30 mT. The [min, max] values are [300, 360 V],  $[0, 5 \times 10^{16} \text{ m}^{-3}]$ , [0, 15 eV], [0, 10 eV], respectively, for (a), (b), (c), and (d). The regions in white are above the maximum. The structure rotates clockwise in  $14.5 \mu\text{s}$ . The central blue disk is the cathode. The anode is the outer cylinder and its voltage is 350 V.

leading to quasiazimuthal electric fields. This potential structure rotates clockwise with a period of  $14.5 \mu\text{s}$ . The potential drop is much sharper at the leading edge and we will call this region the “front” of the instability or the “spoke” or the “azimuthal sheath” in the rest of this Letter.

The cathode sheath thickness [black region around the cathode in Fig. 2(a) or Fig. 2(b)] is about 5 mm, slightly above the value obtained in the 1D simulation of Fig. 1, but the potential drop in the sheath is close to the whole applied voltage, in contrast to the 1D results, where a large potential drop takes place in the plasma. The ion mean kinetic energy at the cathode [not apparent in Fig. 2(d) because of the scale] is about 200 eV, smaller than the applied voltage because of ionization in the sheath and charge exchange collisions (the ion mean free path at 10 mtorr in argon is about 4 mm in the simulations).

The azimuthal rotating sheath is associated with a double layer (positive charge in the leading edge, negative charge in the back) with a total thickness  $s$  of about 5 mm. The maximum azimuthal electric field  $E_\theta$  in the front is therefore on the order of  $10^4 \text{ V/m}$  ( $E_\theta = 2U/s$  with  $U \approx 25 \text{ V}$ ). Ions are accelerated in the azimuthal sheath [Fig. 2(d)], leading to a depletion of the plasma density in the front region [Fig. 2(b)]. The maximum energy reached by the ions in the azimuthal sheath is about 5 eV, which is lower than the potential drop because ions created in the ionization front do not “see” the total potential drop and because of charge exchange collisions. The large azimuthal sheath field in the front generates an  $E_\theta \times B$  drift, i.e., an electron flow along the sheath (perpendicular to the sheath field and almost radial), which can be seen in Fig. 3(a). The  $E_\theta \times B$  electron current is perpendicular to the electric field thus parallel to the equipotential lines as seen in Fig. 3(a). Note that the electron flow in the front is directed from anode to cathode and is the continuation of the

azimuthal component of the electron flow in the anode sheath [see the arrows in Fig. 3(a)]. Of course the net electron flow must be directed from cathode to anode. Most of the electron current to the anode [Fig. 3(a)] is an  $E_\theta \times B$  flow in the azimuthal field at the rear end of the lower potential region of the plasma. Since the azimuthal potential gradient is smaller in this region (and in opposite direction) than in the front, the  $E_\theta \times B$  electron current density is lower than in the front but is distributed over a much larger region.

Electrons are heated during their drift along the anode sheath and the azimuthal sheath as can be inferred from the enhanced mean electron energy and ionization rate in these regions [Figs. 2(c) and 3(b)]. This heating can be due to classical collisional transport across the sheaths or to wave particle interaction. Collisional heating is significant in our conditions as discussed below. Consider an electron drifting along the sheath (anode or azimuthal) over a length  $L$ . Since the ratio of the collisional velocity along the  $E$  field to the  $E \times B$  velocity is equal to  $1/h$  ( $h$  is the Hall parameter), the energy gain along  $E$  during an  $E \times B$  drift of length  $L$  is  $EL/h$ . Since in our conditions  $E \approx 10^4 \text{ V/m}$  and  $h \approx 10^2$  the energy gain during an  $E \times B$  drift of  $L = 1 \text{ cm}$  is 1 eV. Therefore electrons drifting in the anode sheath and entering the azimuthal sheath have undergone significant collisional heating and this appears to be sufficient to increase the ionization rate in the sheath regions. Collisionless heating could also contribute to the overall electron heating in the azimuthal sheath. The electric potential and electron temperature displayed in Figs. 2(a) and 2(c) show the development of instabilities during electron transport along the azimuthal sheath. These are likely to be two-stream instabilities but their contribution to electron heating does not appear to be significant in our conditions. Note that the two-stream heating mechanism proposed in the CIV literature [4] is based on oscillations along the magnetic field, which are not described in the present 2D simulation.

Figure 4 shows the variations of the electric potential, electron mean energy, and ion mean energy along the azimuthal direction at a fixed radius of 2 cm and the radial and azimuthal components of the electron current density in the anode sheath.

We see on Fig. 4(a) the sharp increase of the potential and mean electron energy in the azimuthal sheath. As mentioned above, electron transport to the anode takes place in the region after the front, where the potential goes up and the azimuthal field changes sign. This is confirmed in Fig. 4(b) which displays the radial and azimuthal components of the electron current density along the azimuthal direction in the anode sheath. The ion mean energy in the ionization front is maximum at the end of the azimuthal sheath [Fig. 4(a)] and on the order of 5 eV. This corresponds to a velocity of 4.9 km/s. A  $2\pi$  rotation of the structure takes place in  $14.5 \mu\text{s}$ . The velocity of a point at a

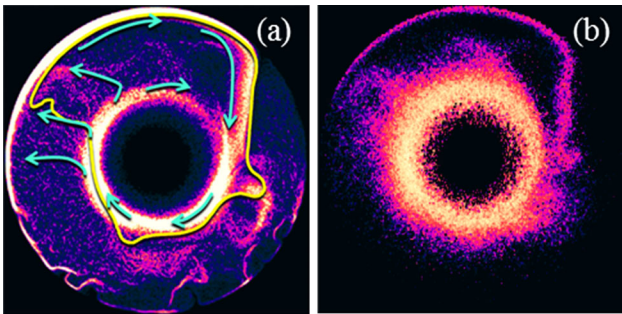


FIG. 3 (color online). Space distributions of (a) the electron current density (the arrows indicate the direction of the electron flow, one equipotential line is also represented). (b) The ionization rate in the conditions of Fig. 2. The [min, max] values are  $[0, 25 \text{ A/m}^2]$  for the current density (linear scale), and  $[0, 5 \times 10^{22} \text{ m}^{-3} \text{ s}^{-1}]$  for the ionization rate (log scale, three decades). The peak current density is  $100 \text{ A/m}^2$ . The color bar is the same as in Fig. 2.

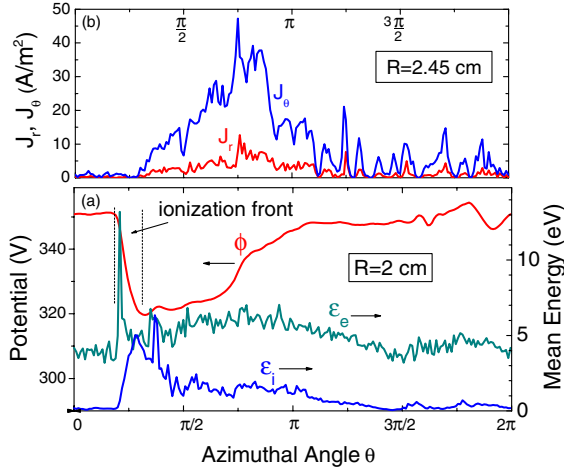


FIG. 4 (color online). (a) Distributions of the electric potential  $\phi$  and mean electron and ion kinetic energy,  $\epsilon_e$  and  $\epsilon_i$ , along the azimuthal direction at a radius  $R = 2$  cm. (b) Distribution of the azimuthal and radial components of the electron current density  $J_\theta$  and  $J_r$  along the azimuthal direction at a radius  $R = 2.45$  cm (anode sheath).  $\theta$  is the angle with the horizontal axis. The front starts slightly before  $\theta = \pi/4$ .

radius  $R = 1$  cm is therefore 4.3 km/s, close to the ion velocity in the azimuthal sheath. The CIV in argon,  $v_c = \sqrt{2eU_i/M}$ , is 8.7 km/s, i.e., about twice larger than the calculated ion velocity in the sheath. Note that the shape of the front, not perfectly azimuthal, must adjust to ensure that the structure rotates as a rigid body.

The properties of the rotating instability as predicted by the PIC MCC simulations and described above are strikingly similar to those of the rotating structures described in the abundant literature devoted to the critical ionization velocity introduced by Alfvén [2,3]. The model of Piel, Möbius, and Himmel [4], for example, is based on the assumption that the moving instability is an electrostatic sheath sustained by ionization (ionization front) where electrons, subject to  $E_\theta \times B$  along the sheath, are heated by a two-stream instability. The simulations are consistent with the general picture of the instability provided by the model of Piel, Möbius, and Himmel, but two points need clarification. The first one is that the sheath motion in the model of Piel, Möbius, and Himmel is directed towards the lower potential region. This is the opposite in our conditions since the radial electron flow in the ionization front must connect with the clockwise azimuthal flows in the cathode and anode sheaths as seen in Fig. 3(a). The second point concerns the mechanism of electron heating. The simulations show that in our conditions, collisionless electron heating is not required to maintain the ionization front (although wave instabilities develop in this region, as observed in the experiments).

Another important aspect of the experiments was the measurements of the radial potential drop in the plasma

$\delta U_p$  (the “burning voltage”) defined above and the demonstration [2,3] that  $\delta U_p$  was limited and close to  $v_c B d$ .  $\delta U_p$  was up to 1 kV in the experiments. In our conditions, the magnetic field  $B$  and the gap length  $d$  are both about 10 times lower than in these experiments so  $\delta U_p$  is small, less than 10 V [see Fig. 2(a)], i.e., smaller than the anode sheath voltage and difficult to define precisely. It is therefore difficult to conclude that the model results confirm the experimental findings on this point. On the other hand, the simulation results for different gases (not shown here) show that the rotation velocity of the spoke decreases with increasing atom mass as  $M^{-1/2}$ , which is consistent with the CIV.

Finally, we must note that the fact that the plasma radial electric field in the CIV experiments and in this Letter is not larger than  $\delta U_p/d = v_c B$  is not a general feature of cross-field devices. It is well known that much larger fields can be established across a magnetic field, e.g., in a Hall thruster. The simulations show that the instability described in this Letter can be suppressed if the magnetic field is not uniform and if its profile is adjusted in a proper way. These results will be presented in a forthcoming paper.

In summary, we have shown for the first time on the basis of a self-consistent kinetic simulation, evidence of the formation of a rotating ionization front (spoke) whose properties are qualitatively very similar to those studied in experiments related to the Alfvén’s critical ionization velocity. This rotating structure is generated when driving a current by applying a voltage across a uniform magnetic field. Instabilities of the Simon-Hoh type prevent the establishment in the plasma of the large radial electric field that would be necessary to transport the electron current in a purely classical, collisional way across the magnetic field. The system finds a stable, rotating solution where the plasma is azimuthally separated in two regions at different electric potentials, with a sharp potential drop at the front. This sharp boundary defines an azimuthal ionization front (spoke) that moves in the direction of the higher potential. The large  $E_\theta \times B$  electron current flowing from anode to cathode in the front is subject to a two-stream instability. This instability is not the dominant electron-heating mechanism in the simulation (collisional heating appears to be sufficient).  $E_\theta \times B$  electron transport from cathode to anode is ensured in the back of the lower potential structure where the azimuthal field is lower and in a direction opposite to that in the front.

These results provide a new insight in the physics of plasma transport in cross-field devices and suggest that the rotating instabilities observed in the relatively complex and high-current plasma experiments designed in the context of CIV studies, should also be observed in much simpler conditions such as those of low current cylindrical magnetron discharges.

- 
- [1] H. Alfvén, *On the Origin of the Solar System* (Oxford University Press, New York, 1954).
- [2] A. Piel, *Adv. Space Res.* **10**, 7 (1990).
- [3] N. Brenning, *Space Sci. Rev.* **59**, 209 (1992).
- [4] A. Piel, E. Möbius, and G. Himmel, *Astrophys. Space Sci.* **72**, 211 (1980).
- [5] N. Brenning, D. Lundin, T. Minea, C. Costin, and C. Vitelaru, *J. Phys. D* **46**, 084005 (2013).
- [6] J.P. Boeuf, B. Chaudhury, and L. Garrigues, *Phys. Plasmas* **19**, 113509 (2012).
- [7] A.V. Phelps database, <http://www.lxcat.laplace.univ-tlse.fr> (retrieved 09 August 2013).
- [8] T. van der Straaten, T. Cramer, I. Falconer, and B. James, *J. Phys. D* **31**, 177 (1998).
- [9] A. Simon, *Phys. Fluids* **6**, 382 (1963).
- [10] F.C. Hoh, *Phys. Fluids* **6**, 1184 (1963).
- [11] Y. Sakawa, C. Joshi, P.K. Kaw, V.K. Jain, T.W. Johnston, F.F. Chen, and J.M. Dawson, *Phys. Rev. Lett.* **69**, 85 (1992).